

Realistic calculation of the low- and high-density liquid phase separation in a charged colloidal dispersion

S. K. Lai,^{1,2} W. P. Peng,¹ and G. F. Wang¹

¹*Complex Liquids Laboratory, Department of Physics, National Central University, Chung-li 320, Taiwan, Republic of China*

²*Physical and Theoretical Chemistry Laboratory, Oxford University, Oxford, OX1 3QZ, United Kingdom*

(Received 10 October 2000; published 29 March 2001)

A realistic statistical-mechanics model is applied to describe the repulsive interaction between charged colloids. The latter, in combination with the long-range van der Waals attraction simulated under excess salt environment, gives rise to a total intercolloidal particle potential showing a clear second potential minimum. Differing from the usual Derjaguin-Landau-Verwey-Overbeek (DLVO) model, the present model is valid at any finite concentration of colloids and is thus an appropriate model for investigating the low- and high-density liquid phase transition. Employing this two-body colloid-colloid potential and in conjunction with the Weeks-Chandler-Andersen [J. D. Weeks, D. Chandler, and H. C. Andersen, *J. Chem. Phys.* **54**, 5237 (1971)] thermodynamic perturbation theory, we derive analytical expressions for the pressure, chemical potential, and related thermodynamic functions. These thermodynamic quantities were used to calculate the phase diagrams of charged colloidal dispersions in terms of the critical parameters: temperature, volume fraction, and electrolyte concentration parameter k_D . Compared with the DLVO model, we find the areas enclosed within the spinodal decomposition and also the liquid-liquid coexistence curves broader in the present model for an excess salt condition $\kappa = k_D \sigma_0 \leq 200$, σ_0 being the macroion diameter, in addition to exhibiting a shift in the critical point κ_c to lower values; for $\kappa > 300$, the disparities between the two models reduce. The same thermodynamic perturbation theory has been employed to study also the weak reversible coagulation whose physical origin is attributed to the presence of the second potential minimum. We examine various colloidal parameters that affect the structure of the latter and deduce from our analysis the conditions of colloidal stability. In comparison with the measured flocculation data for a binary mixture of polystyrene lattices and water, we find that our calculated results are generally reasonable, thus lending great credence to the presently used model.

DOI: 10.1103/PhysRevE.63.041511

PACS number(s): 64.70.Ja, 67.40.Kh, 61.43.Hv, 82.70.Dd

I. INTRODUCTION

A charged colloidal suspension comprises a dispersive host, which consists of macroions in thermal equilibrium with their dissociated counterions and both species are immersed in a dispersive medium such as water. For highly charged macroions, the Coulomb interactions between colloidal particles are often complicated by the oppositely charged counterions, since the number density of counterions is generally very large. The complexity of these multicomponent species will be further increased by the addition of salts (coions) particularly for polyvalent electrolytes. Fortunately, for most charged colloidal dispersions, the macroion size, characterized by the hard-sphere diameter σ_0 , is much larger than that of the surrounding small ions (counterions and salt) and this property of size disparity has greatly simplified theoretical analysis. In fact in the extreme limit of pointlike small ions and within the context of the mean spherical approximation (MSA), an exact repulsive intermacroion Yukawa potential, $\phi(x) = \Lambda \exp[-\kappa(x-1)]/x$, $\kappa = k_D \sigma_0$ being the reduced Debye Hückel wave number, has recently been derived [1,2]. There are two main characteristics of this $\phi(x)$ that differentiate it from the widely used DLVO model [3]. The first characteristic is the derived coupling constant Λ , which depends on the macroion volume fraction η and, as a result, the model is appropriate for studying colloidal dispersions ranging from a lower-density “liquid” phase (an analog of a gas) to a higher-density liquid

phase. This feature is in marked contrast to the DLVO potential, where the Λ is η independent and, strictly speaking, the DLVO model should be useful only for a dilute colloidal solution. The second characteristic is on the spatial correlations and the electrostatic response of the small ions to charged macroions. Both effects are approximately but reasonably incorporated through the coupling coefficient Λ and the screening parameter κ . This effective one-component macrofluid model $\phi(x)$ has been proposed independently earlier by Belloni [1] and a year later by Khan, Morton, and Ronis [2]. The two models were compared favorably [4] with accurate numerical solutions of the hypernetted-chain method for the structures of charged colloids. The model of Belloni, in particular, has been successfully applied to interpret the micelle static structure factor [5] and to predict the liquid-glass transition phase diagram [6]. Remarkably good agreement with measured data has prompted us to proceed, in this paper, to a more quantitative evaluation of the model. The purpose of this paper is to apply the model to study the problems of phase equilibria, focusing in particular on the widely discussed “second minimum” of the total interaction potential $V(r)$ that leads to the liquid-liquid phase separation.

The existence of a second minimum in the intercolloidal particle potential $V(r)$ has been an issue of continual interest. In their classic monograph, Verwey and Overbeek [3] discussed the phenomenon of coagulation drawing attention to the London-van der Waals attractive interaction as the possible cause for the occurrence of a second minimum in $V(r)$ that gives rise to the weak reversible coagulation. Vari-

ous controlled parameters pertaining to a charged colloidal dispersion such as the σ_0 , κ , Hamaker constant A , surface potential Ψ , etc., have been measured and varied, and these were analyzed using the simplified model of DLVO theory to show the change in $V(r)$, in particular the magnitude $V(r_m)$ at the second minimum position r_m and the accompanied potential barrier height lying between the primary minimum and r_m . Since this pioneering work, experimental efforts in understanding the second minimum of spherical charged colloids as a possible mechanism for the weak reversible coagulation have been carried out independently by Schenkel and Kitchener [7], Long, Osmond, and Vincent [8], Kotera, Furusawa, and Kubo [9], and more recently by Gotoh *et al.* [10]. Theoretically, Grimson [11] proposed a simple mean-field theory to study the phase separation of a weakly charged colloidal dispersion. His results have been criticized by Victor and Hansen [12] to be inadequate for quantitative studies of phase equilibria. Victor and Hansen subsequently advanced a first-order thermodynamic perturbation theory and showed from calculated phase diagrams the possibility of predicting the weak reversible coagulation in terms of the $V(r_m)$. Their work has been extended by Kaldasch, Laven, and Stein [13] to second-order correction and included studies of the liquid-solid coexistence phases. Since the works of Victor and Hansen and of Kaldasch, Laven, and Stein, there appears to be no further theoretical work in the literature [14] devoted to studying the mechanism of the second minimum on the phase separation at the same level of quantitative analysis. It is therefore of great theoretical interest to revisit this problem given that a many-body statistical-mechanics means of calculating the charged intercolloidal particle interaction has emerged and the constructed $V(r)$ interprets accurately and reliably [4,5] the charge-stabilized colloidal structures.

Our motivation for this paper is twofold. First, we shall apply the Belloni model to the study of phase separation. Differing from the DLVO model, the Belloni model includes somewhat quantitatively the statistical-mechanics property in the intercolloidal particle potential. The latter is manifested by its coupling strength depending explicitly on η whose limit $\eta \rightarrow 0$ is the DLVO model. Second, we shall, wherever possible, compare the calculated results with experiments to reveal the potential usefulness of the present method. Hopefully this will stimulate further experimental endeavors. The paper is therefore organized as follows. In the next section, we give a brief account of the repulsive potential between two colloidal particles stressing the statistical-mechanics feature. Then, we add to this repulsive force the London-van der Waals attractive potential. The total interaction potential in conjunction with the Weeks-Chandler-Andersen (WCA, [15]) thermodynamic perturbation theory is then employed to construct an equilibrium colloidal Helmholtz free energy. Our numerical results are presented in Sec. III for (a) the spinodal decomposition, (b) the liquid-liquid phase separation, and (c) the phase diagrams that can be used to understand the colloidal stability. We deduce from (c) our calculated critical colloidal parameters and they are compared with early experiments of Kotera, Furusawa, and Kubo [9] whose colloidal conditions closely mimic the ones discussed

here. It appears that considerable improvement can be achieved in bridging theory and experiment if further refinement of the present theory is made. Finally, we summarize in Sec. IV all of our calculated results.

II. THEORY

In this section, starting with the theory of integral equation, we construct an effective interparticle potential for two charged colloidal particles. Then, following closely the work of Victor and Hansen [12], we apply the WCA perturbation theory [15] to calculate the Helmholtz free energy of a charged colloidal dispersion.

A. Total potential energy

Let us begin with the multicomponent Ornstein-Zernike (OZ) equations given by

$$h_{ij}(r) = c_{ij}(r) + \sum_{l=0} \rho_l \int h_{il}(|\mathbf{r}-\mathbf{r}'|) c_{lj}(r') d\mathbf{r}', \quad (1)$$

where ρ_l is the number density and species i, j , and l are defined as $i, j, l=0$ for macroions, $i, j, l=1$ for counterions, and $i, j, l=2, 3, \dots$ for other small ions such as an added electrolyte. In Eq. (1) $c_{ij}(r)$ is the direct correlation function and $h_{ij}(r) = g_{ij}(r) - 1$ is the total correlation function written in terms of the pair-correlation function $g_{ij}(r)$. It was shown by Adelman [16] that the small ions (counterions and coions) in Eq. (1) can be neatly integrated to yield a one component OZ equation for the macroions whose effective direct correlation function $c_{00}^{\text{eff}}(r)$ satisfies

$$h_{00}(r) = c_{00}^{\text{eff}}(r) + \rho_0 \int h_{00}(|\mathbf{r}-\mathbf{r}'|) c_{00}^{\text{eff}}(r') d\mathbf{r}'. \quad (2)$$

Denoting the Fourier transform of $c_{00}^{\text{eff}}(r)$ by $\hat{c}_{00}^{\text{eff}}(q)$, it can be shown further [1,4] that

$$\hat{c}_{00}^{\text{eff}}(q) = \hat{c}_{00}^s(q) + \sum_{i=1} [\hat{c}_{0i}^s(q)]^2 - \frac{[\alpha_0 + \sum_{i=1} \alpha_i \hat{c}_{0i}^s(q)]^2}{q^2 + k_D^2}, \quad (3)$$

where the $\hat{c}_{ij}^s(q)$ is the short-range part of $\hat{c}_{ij}(q)$, $k_D^{-1} = 1/\sqrt{\sum_{i=1} \alpha_i^2}$ is the Debye Hückel screening length, and $\alpha_i^2 = 4\pi L_B \rho_i Z_i^2$, L_B and Z_i being the Bjerrum length and the charge of a macroion or a small ion, respectively. By treating the small ions as pointlike particles, an analytical formula for the inverse Fourier transform of Eq. (3) can be obtained [1,4] leading to

$$c_{00}^{\text{eff}}(r) = -Z_0^2 L_B X^2 \exp[-k_D(r - \sigma_0)] \frac{\exp[-k_D(r - \sigma_0)]}{r}, \quad r > \sigma_0, \quad (4)$$

where the coupling parameter

$$X = \cosh\left(\frac{\kappa}{2}\right) + U \left[\frac{\kappa}{2} \cosh\left(\frac{\kappa}{2}\right) - \sinh\left(\frac{\kappa}{2}\right) \right], \quad (5)$$

in which are buried the correlations between macroions and small ions, depends not only on κ but also on $\eta = \pi\rho_0\sigma_0^3/6$ through $U = (8\zeta/\kappa^3 - 2\nu/\kappa)$ in which $\zeta = 3\eta/(1-\eta)$, $\nu = (\Gamma_\sigma + 2\zeta)/[2(1+\zeta) + \Gamma_\sigma]$, and

$$(\Gamma_\sigma^2 - \kappa^2)[2(1+\zeta) + \Gamma_\sigma]^2 = 96\eta(Z_0^2/\sigma_0)L_B. \quad (6)$$

Given Z_0^2/σ_0 , κ , and η , Eq. (6) has to be solved for Γ_σ and hence X in Eq. (5). It is easy to show that $X \rightarrow \exp(\kappa/2)/(1 + \kappa/2)$ in the limit of $\rho_0 \rightarrow 0$, a linearized DLVO result. This implies that the present model is appropriate for the description of a suspension of charged colloids at any finite concentration.

We turn now to a discussion of the result of Eq. (4). First of all, we recall from the literature [17] that the pair distribution function $g(r)$ can be defined quite generally in terms of the two-body colloid-colloid potential of mean force $\phi(r)$ by the relation

$$g(r) = \exp[-\beta\phi(r)], \quad (7)$$

where $\beta = 1/(k_B T)$ is the inverse temperature. If we compare Eq. (7) with the hypernetted-chain closure (known to be highly accurate for Coulomb liquids) which is given exactly by

$$g(r) = \exp[h(r) - c(r) - \beta v(r)], \quad (8)$$

we deduce by appealing to Eq. (2) that $\beta\phi(r) = -\rho_0 \int h(|\mathbf{r} - \mathbf{r}'|)c(r')d\mathbf{r}' + \beta v(r)$; the $v(r)$ is therefore a *direct* two-particle potential (such as the low-density DLVO potential) and the $\phi(r)$ is thus to be interpreted as a potential of mean force for any two particles separated a distance r in thermal equilibrium with all the other particles that play the role of contributing *indirectly* to $\phi(r)$. In the widely used DLVO model in which $\rho_0 \rightarrow 0$ the one-component OZ equation of Eq. (2), will be described quite well by $h^{\text{DLVO}}(r) \approx c^{\text{DLVO}}(r)$. Since $h^{\text{DLVO}}(r) = g^{\text{DLVO}}(r) - 1$, and that in the limit $\rho_0 \rightarrow 0$, $g^{\text{DLVO}}(r) \approx \exp[-\beta v(r)]$. Linearizing the latter function yields $h^{\text{DLVO}}(r) \approx \exp[-\beta v(r)] - 1 \approx -\beta v(r) = c^{\text{DLVO}}(r)$, which is none but the MSA closure. In view of this, it is natural to write Eq. (4) as $c_{00}^{\text{eff}}(r) = -\beta\phi(r)$ and interpret $\phi(r)$ to be an effective two-body potential of mean force, for the X in $\phi(r)$ depends on η and hence includes indirect contributions, albeit approximately (in the sense of utilizing the MSA closure in calculating the various correlations between the macroparticles and small ions). We thus see at this point that by setting $c_{00}^{\text{eff}}(r) = -\beta\phi(r)$ in Eq. (4), we are in fact establishing a more realistic repulsive potential $\phi(r)$ for charged macroparticles. The total potential energy of interaction between two charged colloidal particles is then

$$V(r) = \phi(r) + v_{vdw}(r), \quad (9)$$

where, expressed in reduced distance $x = r/\sigma_0$,

$$v_{vdw}(x) = -\frac{AH(x)}{12} \quad (10)$$

is the van der Waals attraction [3] with

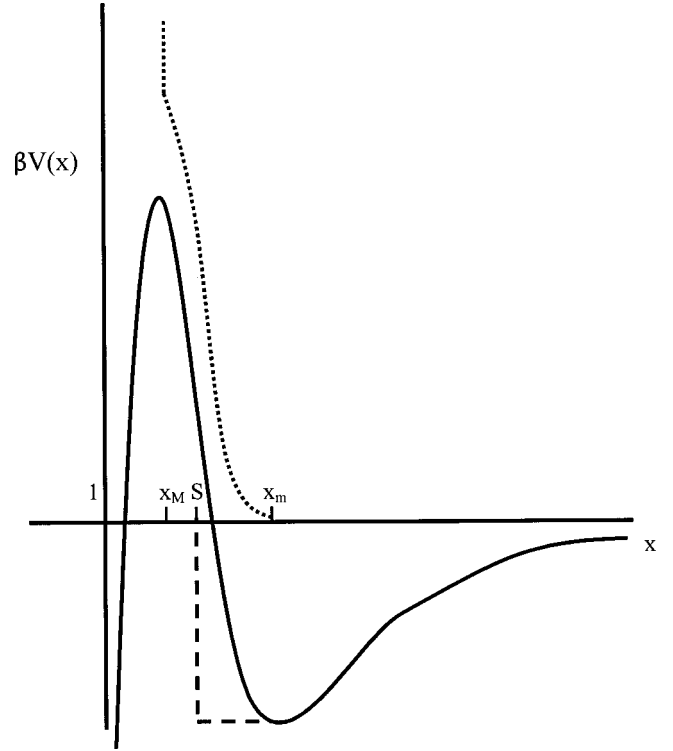


FIG. 1. Schematic diagram for a suspension of charged colloids in the presence of an excess electrolyte. The positions of extrema are the x_M at the potential barrier and the x_m at the second minimum.

$$H(x) = \frac{1}{x^2 - 1} + \frac{1}{x^2} + 2 \ln\left(1 - \frac{1}{x^2}\right). \quad (11)$$

and A is the Hamaker constant. Note that the use of $\phi(r)$ as our repulsive potential for the charged colloidal dispersion is physically more realistic than the DLVO counterpart since the coupling constant X is η dependent and is appropriate for studying phase equilibrium properties such as the (low-density) liquid-(high-density) liquid phase separation.

B. Week-Chandler-Andersen perturbation theory

For convenience in the following discussion, we rewrite Eq. (9) in the form

$$V(x) = \Lambda \left(\frac{\exp[-\kappa(x-1)]}{x} - \frac{AH(x)}{12\Lambda} \right) = \Lambda \varphi(x), \quad (12)$$

where $\Lambda = Z_0^2 L_B X^2 e^{-\kappa}$ in the present model. To apply the WCA perturbation theory, we first split $V(r)$ into two parts, a repulsive v_r and an attractive v_a ; the former constitutes a reference system, while the latter is treated as a perturbation. For the charged colloidal dispersion, the separation is done as follows. In the first place, we note that the structure of $V(x)$ for an excess salt constant $\kappa \gg 1$ changes asymptotically from a negative $V(x)$ to a (second) minimum $V(x_M)$, continues further to a positive maximum barrier $V(x_m)$, and then crosses over to an infinitely deep (first) minimum. Figure 1 displays schematically a typical structure of $V(x)$. The

extrema $V(x_m)$ and $V(x_M)$ can be easily determined by the condition $V'(x)=0$, which leads

$$e^y - \gamma y^2 \left(1 + \frac{y+1}{\kappa}\right) \left(1 + \frac{y}{\kappa}\right) \left(1 + \frac{y}{2\kappa}\right)^2 = 0, \quad (13)$$

where $y = \kappa(x-1)$ and $\gamma = 24\Lambda/(A\kappa)$. The existence of the extrema has two immediate consequences, which have been investigated experimentally. At the second minimum position x_m , it was observed by Kotera, Furusawa, and Kubo [9] and others [7,8] that a charged colloidal solution would undergo a reversible coagulation. The characteristic depth of the potential well ranges from a few $k_B T$ to approximately $15 k_B T$. For such a phenomenon to be realized, the potential barrier $V(x_M)$ at the x_M must also be high in order to prevent the energetic colloids falling into the primary minimum at which place an irreversible coagulation occurs. Experimental works on polystyrene charged latices in water [7,9] indicate that an order of $V(x_M) \approx 15 k_B T$ would be sufficient for observing less unambiguously the weak reversible coagulation. In view of this global structure of $V(x)$, it is natural to write

$$V(x) = v_r(x) + v_a(x) \quad (14)$$

and choose the repulsion

$$\begin{aligned} v_r(x) &= \infty, & x < x_M, \\ &= V(x) - V(x_m), & x_M < x < x_m, \\ &= 0, & x > x_m, \end{aligned} \quad (15)$$

as the reference system and treat the attraction

$$\begin{aligned} v_a(x) &= 0, & x < x_m, \\ &= V(x), & x > x_m, \end{aligned} \quad (16)$$

as a perturbation. Now, in the WCA theory, one can take advantage of the strong Coulomb repulsion for charged colloidal particles and make reasonable approximation on the reference part. As displayed schematically in Fig. 1, the $V(x)$ in the range $x_M < x < x_m$ is rather steep and this prompts us to consider replacing the v_r by

$$\begin{aligned} v_S(x) &= \infty, & x < S, \\ &= 0, & x > S, \end{aligned} \quad (17)$$

which is a fluid of equivalent hard spheres characterized by a size $\sigma = S\sigma_0$, $S > 1$ being a dimensionless constant measuring the ‘‘softness’’ of the macroparticles. This approximation on v_r , in turn, will lead us to rewrite Eq. (16) as

$$\begin{aligned} v_a(x) &= 0, & x < S, \\ &= V(x_m), & S < x < x_m, \\ &= V(x), & x > x_m. \end{aligned} \quad (18)$$

For a given density ρ_0 , the volume fractions $\eta = \pi\sigma^3\rho_0/6$ and $\eta_0 = \pi\sigma_0^3\rho_0/6$ are accordingly related by $\eta = S^3\eta_0$.

Now, it was shown in Ref. [18] that the reference free energy can be calculated by carrying out a functional Taylor series expansion in $\Delta = \exp[-\beta v_r(x)] - \exp[-\beta v_S(x)]$. Keeping to first order in Δ , the S can be determined by the equation:

$$\int_0^\infty B(x)x^2 dx = 0, \quad (19)$$

where the ‘‘blip function’’

$$B(x) = Y_\eta(x)\Delta. \quad (20)$$

The function $Y_\eta(x)$ in Eq. (20) is $Y_\eta(x) = \exp[\beta v_S(x)]g_\eta(x)$, $g_\eta(x)$ being the pair-correlation function evaluated at η . Note that $B(x)$ is nonzero only in the range $x_M < x < x_m$ and in conjunction with the fact that both the $Y_\eta(x)$ and its derivative are continuous at the contact point $x=S$, we may perform, as in Verlet and Weis [18], a systematic expansion of $x^2 Y_\eta(x)$ around $x=S$, i.e., in powers of $(x-S)$. The leading term in this expansion leads to the density-independent Barker-Henderson diameter S :

$$S = x_M + \int_{x_M}^{x_m} \{1 - \exp[-\beta v_r(x)]\} dx. \quad (21)$$

This expression for S can be written [18] to vary as $S \approx 1 + s/\kappa + O(1/\kappa^2)$ in which s is a numeric constant. Although we shall be interested in cases of $\kappa \gg 1$, we prefer to retain the exact form for S . Having determined S , the problem of modeling v_r by equivalent hard spheres has, so to speak, been solved, since an analytical solution for the Percus-Yevick hard-sphere Helmholtz free energy f_{hs} is available. Using the compressibility equation of state, one obtains

$$\beta f_{hs} = \frac{3\eta(2-\eta)}{2(1-\eta)^2} + \ln\left(\frac{\eta}{1-\eta}\right) + \ln\left(\frac{\lambda_T^3}{\Omega}\right) - 1, \quad (22)$$

where $\lambda_T = h/\sqrt{2\pi mk_B T}$ is the de Broglie wavelength and $\Omega = \pi\sigma^3/6$ is the effective hard-sphere volume. We should emphasize that, although we have employed the compressibility equation of state to derive f_{hs} , an equally permissible f_{hs} resorting to the energy equation route is also possible, for the Percus-Yevick closure yields just an approximate $g_\eta(x)$.

We come now to the calculation of the first-order correction f_1 added to f_{hs} . In terms of the perturbation $v_a(r)$, f_1 may be written in the high-temperature approximation as

$$f_1 = 12\eta_0 \int_0^\infty dx g_\eta(x) v_a(x) x^2. \quad (23)$$

This so-called high-temperature approximation, which amounts to ignoring the spatial correlation of the attractive perturbation, has been examined by Hansen *et al.* [19] to be accurate enough for colloidal liquids. Following Victor and Hansen [12], Eqs. (18) and (23) can be analytically calculated to read

$$\beta f_1 = - \frac{T_A \eta_0 (1 + \eta/2) [\xi - \alpha(\eta)]}{2T(1-\eta)^2}, \quad (24)$$

where, $T_A = A/k_B$, and

$$\xi = \ln\left(\frac{\kappa}{y_m}\right) - \gamma \kappa \varphi(x_m)(y_m - S) - \gamma \exp(-y_m) \quad (25)$$

in which

$$\alpha(\eta) = \sum_{i=0}^2 \delta_i \eta^i. \quad (26)$$

Here S is the parameter defined in Eq. (21) and δ_i are numerical constants and $y_m = \kappa(x_m - 1)$. Note that, differing from the work of Victor and Hansen [12], the ξ in the present model depends on η through the X in γ .

We are now equipped to calculate the pressure and chemical potential that both are needed for locating the critical points and hence the phase diagrams. Utilizing the Helmholtz free energy $f = f_{hs+f_1}$ [20], we obtain for the pressure

$$\begin{aligned} \beta P \Omega &= \eta_0^2 \frac{\partial(\beta f)}{\partial \eta_0} \\ &= \eta_0 \frac{1 + \eta + \eta^2}{(1 - \eta)^3} - \frac{T_A}{T} \frac{\eta_0^2}{2} \frac{1}{(1 - \eta)^3} \end{aligned}$$

$$\begin{aligned} &\times \left\{ (1 + 2\eta)[\xi - \alpha(\eta)] + \eta(1 - \eta)(1 + \eta/2) \right. \\ &\times \left. \left(\frac{d\xi(\eta)}{d\eta} - \frac{d\alpha(\eta)}{d\eta} \right) \right\} \quad (27) \end{aligned}$$

from which the chemical potential μ can be calculated straightforwardly by $\beta\mu = \beta(f_{hs} + f_1) + \beta P \Omega / \eta_0$. Furthermore, the isothermal compressibility χ_T can be obtained by differentiating Eq. (27) yielding

$$\begin{aligned} (\rho_0 k_B T \chi_T)^{-1} &= \frac{\partial(\beta P \Omega)}{\partial \eta_0} \\ &= \frac{(1 + 2\eta)^2}{(1 - \eta)^4} - \frac{T_A \eta_0}{T} \left\{ \frac{1 + 7\eta/2}{(1 - \eta)^4} [\xi - \alpha(\eta)] \right. \\ &\quad + \frac{\eta(2 + 3\eta/2 - \eta^2/2)}{(1 - \eta)^3} \left(\frac{d\xi(\eta)}{d\eta} - \frac{d\alpha(\eta)}{d\eta} \right) \\ &\quad \left. + \frac{\eta^2(1 + \eta/2)}{2(1 - \eta)^2} \left(\frac{d^2\xi(\eta)}{d\eta^2} - \frac{d^2\alpha(\eta)}{d\eta^2} \right) \right\}, \quad (28) \end{aligned}$$

which on further differentiation leads to

$$\begin{aligned} \frac{\partial}{\partial \eta_0} [(\rho_0 k_B T \chi_T)^{-1}] &= \frac{4\eta}{\eta_0} \frac{(1 + 2\eta)(\eta + 2)}{(1 - \eta)^5} - \frac{T_A}{T} \left\{ \frac{1 + 10\eta + 7\eta^2}{(1 - \eta)^5} [\xi - \alpha(\eta)] + \frac{\eta^4/2 - 2\eta^3 + 10\eta^2 + 5\eta}{(1 - \eta)^4} \left(\frac{d\xi(\eta)}{d\eta} - \frac{d\alpha(\eta)}{d\eta} \right) \right. \\ &\quad \left. + \frac{\eta^4 - 2\eta^3 - 7\eta^2/2}{(1 - \eta)^3} \left(\frac{d^2\xi(\eta)}{d\eta^2} - \frac{d^2\alpha(\eta)}{d\eta^2} \right) + \left[\frac{\eta^3(1 + \eta/2)}{2(1 - \eta)^2} \right] \left(\frac{d^3\xi(\eta)}{d\eta^3} - \frac{d^3\alpha(\eta)}{d\eta^3} \right) \right\}. \quad (29) \end{aligned}$$

We are now ready to calculate the critical points and the loci of points showing the phase separation. The calculated results and their implication will be given in the next section.

III. NUMERICAL RESULTS AND DISCUSSION

This section is devoted to a presentation of our numerical results for phase equilibria followed by an analysis and a discussion of the implication of these data. For concreteness, we confine our calculations to cases meeting as closely as possible to experimental conditions (such as the works of Kotera, Furusawa, and Kubo [9], Watillon and Joseph-Petit [21], Gotoh *et al.* [10] etc.) and employing, if necessary, in our calculations their measured or proposed colloidal parameters as reasonable input data in our theoretical analysis. Our theoretical results, therefore, are experimentally appealing. We believe that our theoretical analysis below should be very useful for a general understanding of the liquid-liquid phase separation in charged colloidal dispersions.

A. Spinodal decomposition

From the formulas given in Secs. II A and II B, we need to specify the parameters Z_0 , σ_0 , κ , and A in order to solve

Eqs. (28) and (29) for the critical volume fraction η_c as well as the critical temperature T_c below which a liquid-liquid phase separation is to be expected. However, experimentally, it is the surface potential Ψ of charged colloids that is often available. We turn therefore to apply the approximate formula $Z_0 = \pi \Psi \epsilon_0 \epsilon \sigma_0 (2 + \kappa)$ [3] for an evaluation of the Z_0 . For a fixed Ψ , the Z_0 , however, has to be obtained self-consistently with the κ appearing in the formula, which must be the same as that in solving Eqs. (13) and (32) (see Sec. III C below). The Ψ is thus an input parameter numerically fixed at $\Psi \lesssim 25$ mV, which is a range of values consistent with the linearization approximation used in our theory. Given these governing parameters for the charged colloidal dispersion, our numerical work proceeds as follows. First, we assign the dispersive host with a monosize $\sigma_0 = 6000 \text{ \AA}$, characterize the dispersive medium by a dielectric constant $\epsilon = 78.5$, set the surface potential $\Psi = 25$ mV, and fix the temperature of our aqueous colloidal dispersion at $T = 293$ K. For convenience in the following discussion and for the purpose of comparing with experiments, it is perhaps more instructive to determine the critical points (η_c, κ_c) rather than (η_c, T_c) since the former is more accessible to laboratory measurement. Technically these two critical pa-

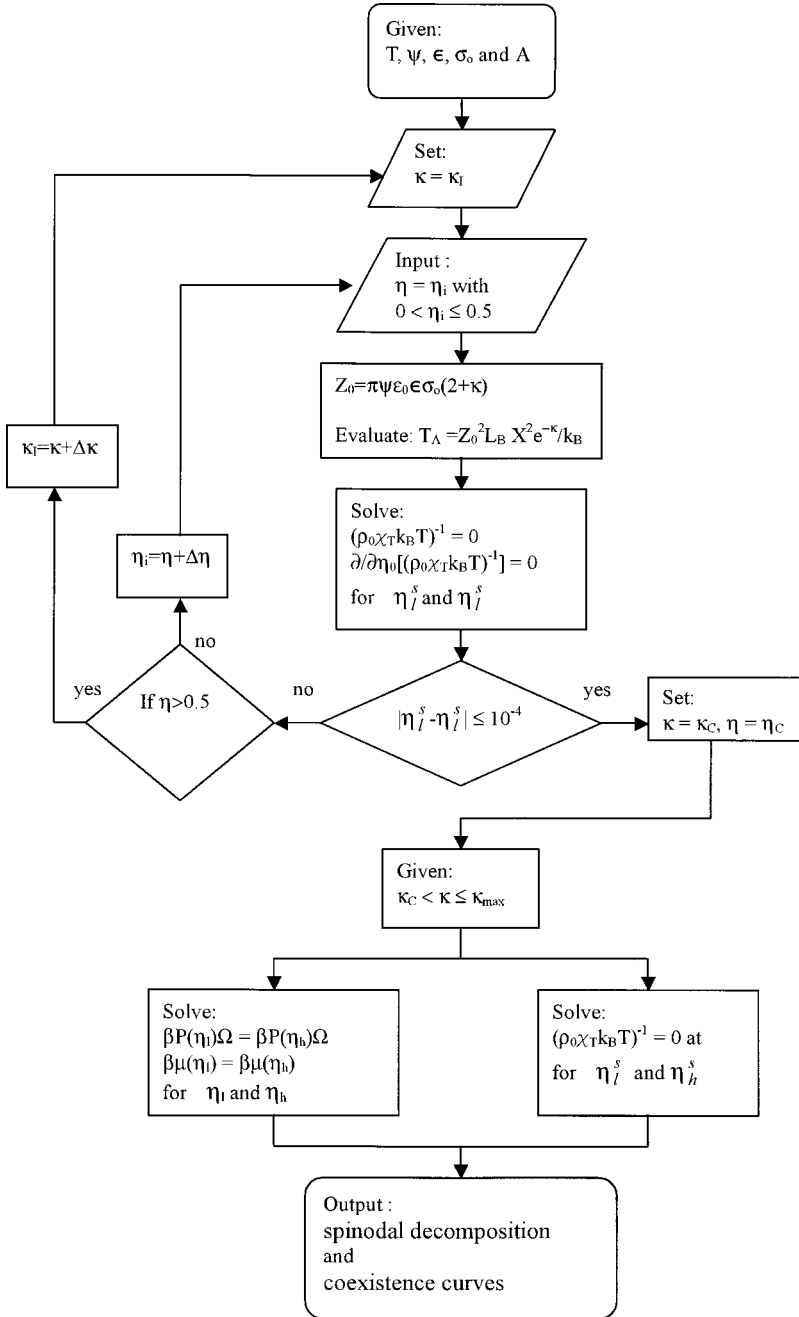


FIG. 2. Flow chart showing the numerical procedure that leads to the determination of the κ_c , η_c , spinodal decomposition, and coexistence curves. The κ_{\max} in the Belloni model is determined as in Fig. 4. Note that for $\eta > 0.5$ the colloidal dispersion has fallen into a solid-phase region.

parameters are obtained by solving Eqs. (28) and (29) for the thermodynamic conditions $(\rho_0 k_B T \chi_T)^{-1} = 0$ and $(\partial/\partial \eta_0) \times [(\rho_0 k_B T \chi_T)^{-1}] = 0$. The spinodal decomposition phase boundary is then obtained by solving Eq. (28) at each $\kappa > \kappa_c$ for the solutions η_l^s and η_h^s following a numerical procedure as detailed in Fig. 2. We should remark at this point that, for given Ψ , the addition of electrolytes will tend to decrease the potential barrier $V(x_M)$ and will eventually drive the charged colloidal dispersion into an unstable irreversible coagulation. This would mean that the κ will be bounded above by a κ_{\max} . For this latter parameter, there are quantitative differences between the Belloni and DLVO models. In the DLVO model the η independence of T_Λ has resulted in a unique κ_{\max} (vs η), the corresponding κ_{\max} in the Belloni model is somewhat complicated by the explicit

dependence of T_Λ on η . It can be shown easily from Eq. (5) that the X generally decreases with increasing η revealing the more dominant role of the geometrical hard-core effect (over the strong Coulomb repulsion). This explains the decrement of κ_{\max} in the Belloni model as the η is increased. We defer to Sec. III C for a more quantitative discussion of the determination of κ_{\max} . Figures 3(a) and 3(b) display our calculated results for a system of monodisperse charged colloids calculated at two different Hamaker constants ($A = 1.3 \times 10^{-20}$ J [9,10] and $A = 3.4 \times 10^{-20}$ J [7]) within the contexts of the Belloni and DLVO models. Quite generally, we observe discernible differences in the spinodal decomposition areas for the two models considered when the excess electrolyte $\kappa \lesssim 200$, whereas for still larger $\kappa > 300$ the disparity is smaller owing to the fact that $X \rightarrow \exp(\kappa/2)/(1$

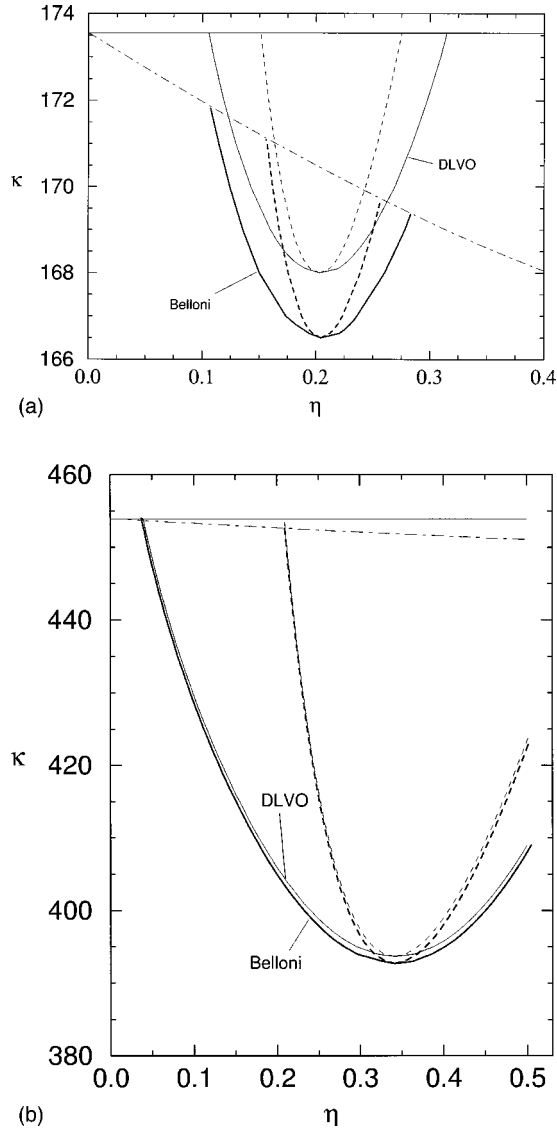


FIG. 3. (a) Spinodal decomposition (Belloni: thick-dashed curve; DLVO: thin-dashed curve) and (low-density) liquid-(high-density) liquid coexistence (Belloni: thick-full curve; DLVO: thin-full curve) curves for an aqueous charged colloidal dispersion at temperature $T=293$ K. The reduced screening parameter is $\kappa = k_D \sigma_0$, k_D and σ_0 being the Debye-Hückel constant and macroion diameter, respectively. Numerical data used are $\sigma_0 = 6000$ Å, $167 < \kappa_{\max} < 172$ (chain curve) [for DLVO, $\kappa_{\max} = 173.56$ (thin-full curve)], Hamaker constant $A = 3.4 \times 10^{-20}$ J, surface potential $\Psi = 25$ mV, $\eta_c = 0.2043$ (0.2033 for DLVO) and $\kappa_c = 166.5$ (168 for DLVO). (b) Same notations as in (a) except $A = 1.3 \times 10^{-20}$ J, $451 < \kappa_{\max} < 453$ (for DLVO, $\kappa_{\max} = 453.9$), $\eta_c = 0.3415$ (0.3415 for DLVO), and $\kappa_c = 392.7$ (393.7 for DLVO).

+ $\kappa/2$) (the DLVO model) in this larger κ limit. The situation $\kappa \lesssim 200$, depicted in Fig. 3(a), corresponds to the case $A = 3.4 \times 10^{-20}$ J, where both models delineate spinodal decomposition curves covering lower η values ($0.15 \leq \eta \leq 0.275$) but predict an almost identical η_c ; quantitatively the spinodal decomposition region (and the critical point κ_c) in the Belloni model is seen to be slightly broader (and lower) compared with the DLVO model. Similar noticeable

disparities mentioned above for the case $A = 3.4 \times 10^{-20}$ J still remain for the situation $\kappa > 300$, shown in Fig. 3(b), which corresponds to the case $A = 1.3 \times 10^{-20}$ J, although the magnitudes of differences are less conspicuous. Note that for this smaller A case the spinodal decomposition curves fall in the higher η values ($0.22 \leq \eta \leq 0.5$).

B. Liquid-liquid coexistence

Having determined the critical points (η_c, κ_c) , it is straightforward to calculate the liquid-liquid coexistence curve by the standard formulas:

$$\beta P(\eta_l)\Omega = \beta P(\eta_h)\Omega, \quad (30)$$

$$\beta \mu(\eta_l) = \beta \mu(\eta_h). \quad (31)$$

Here the low- and high-liquid densities are, respectively, characterized by volume fractions η_l and η_h , which are solutions to the above coupled equations. Given the same set of parameters (σ_0, A, Ψ) as in Sec. II A, Fig. 2 shows also the numerical procedure leading to the physical roots η_l and η_h , which are solved at each $\kappa > \kappa_c$ for the aqueous charged colloids at $T = 293$ K. The liquid-liquid coexistence curves are included in the same Figs. 3(a) and 3(b). Together with the spinodal decomposition curves, the areas in between describe the metastable thermodynamic states, customarily termed the supercooled liquids.

C. Irreversible and reversible coagulation

We turn in this section to the study of the phase separation in charged colloidal solutions. To this end, we calculate the phase diagrams, which can be used to gloss over the coagulation phenomena in a general and realistic way. Let us start with Eq. (12) for the colloid-colloid potential. If the potential barrier $V(x_M)$ is sufficiently high, the resulting colloidal dispersion is in a charge-stabilized equilibrium phase revealing a distribution of charged colloidal particles thermodynamically prevented from an irreversible coagulation. On the other hand, when $V(x_M) = 0$, one would anticipate the charged colloids showing an irreversible coagulation characterized by colloidal particles thermally collided to fall aggregately into the deep primary minimum. Thus, as one lowers the $V(x_M) \gg k_B T$ (for example, by adding an excess electrolyte or by decreasing the Ψ) which corresponds to weakening the strong Coulomb repulsion in a charge-stabilized dispersion, one is in fact enhancing the chance for charged colloids to sample contact configurations. On further lowering the $V(x_M)$, a stage will emerge where the interaction of charged colloidal particles, due to increasingly high possibility of particles coming close to each other, begins to be operated jointly by the Coulomb repulsive force and the London-van der Waals attraction, leading in this case to the appearance of a second minimum $V(x_m)$ in the potential function $V(x)$ (see the full curve in Fig. 1). Depending on the values σ_0 and A , the $V(x_m)$ varies in magnitude from a value, for microscopic particle ($\sigma_0 \sim 300 - 3000$ Å) [7], generally of the order of $1 \sim 10 k_B T$ [3,7,8,22] to a value, for larger σ_0 (≥ 4500 Å), of the order of $V(x_m) > 10 k_B T$ [9,10].

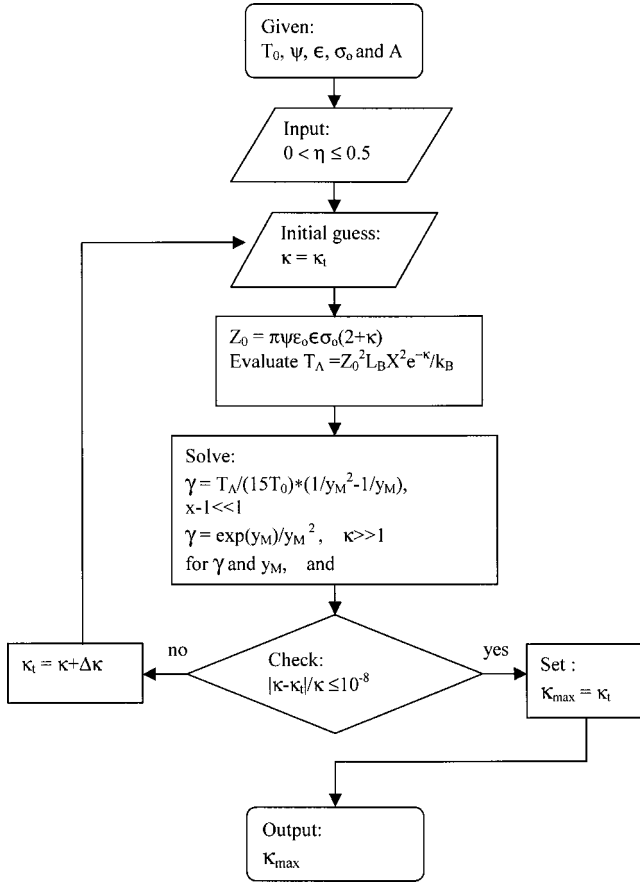


FIG. 4. Flow chart showing the numerical procedure that leads to the determination of the κ_{\max} in the Belloni model (see text).

In particular the second minimum position of the former is generally located at a larger x_m compared with the latter whose x_m is located distinctly nearer to the contact distance $r = \sigma_0^+$. A subtle and delicate matching of the $V(x_M)$ and $V(x_m)$ is thus an important criterion for realizing the reversible coagulation. Such a coagulation condition on charged spherical colloids, deduced from the property of $V(x)$, has in fact been employed by experimentalists [7,9,10] to interpret the observed signature of the reversible coagulation. The question now is: what are the magnitudes of $V(x_M)$ and $V(x_m)$ for a liquid-liquid phase separation to happen, knowing that all of the parameters Z_0, σ_0, κ , and A can influence $V(x)$? In view of the difficulties in stipulating an unambiguous criterion, we have chosen $V(x_M) \approx 15 k_B T$ [23] whose value is selected in consultation with previous experiments [3,7,8,9,10,22]. Subject to this constraint, Eq. (12) reads

$$\varphi(y_M) \approx \exp[-y_M] - \frac{1}{\gamma y_M} = \frac{15T_0}{T_\Lambda}, \quad (32)$$

where $T_\Lambda = \Lambda/k_B$, y_M is the solution of Eq. (13), and T_0 is a temperature to be discussed further below. As depicted in Fig. 4, Eqs. (13) and (32) lead to a minimum value of γ and hence [by the relation $\kappa = 24T_\Lambda/(\gamma T_A)$] a maximum κ_{\max} for a given set of (A, T_Λ) values. These parametric values for the y_M and κ_{\max} imply that a useful parametric space for

studying the liquid-liquid phase separation is to establish a relation between the T_Λ and T_A . The former, at fixed parameters κ and Ψ , is a function of σ_0 and η , while the latter, which correlates closely the stability information of the colloidal dispersion, affects sensitively the structure of $V(x)$ near $x \approx x_m$ [10]. There is, however, one important point that deserves paying attention to. Since water freezes at $T = 273$ K, the calculation of the phase diagram T_Λ vs T_A has to be performed to yield a physically acceptable value of $T_c \geq 273$ K in addition to making sure that its magnitude is not exceedingly large that $k_B T_c > V(x_M)$. Bearing this in mind and considering the possibility of correlating the calculated results with measurements (such as those reported by Kotera, Furusawa, and Kubo [9]), we have therefore set $T_0 = T_c = 293$ K. Now, to locate the loci of the $T_\Lambda - T_A$ phase boundary, it is more convenient to input T_A and solve for the T_Λ and η_c from Eqs. (28) and (29). For the T_A values, they are reasonably selected from the empirical range $500 \text{ K} < T_A \leq 10^4 \text{ K}$ [24]. This numerical procedure differs from that of Victor and Hansen [12], for the T_Λ in the Belloni model depends on η whose critical value η_c has to be obtained self-consistently as detailed in the flow chart of Fig. 5. Figure 6 shows our determined T_Λ vs T_A compared with the DLVO results calculated under the same colloidal conditions.

Let us scrutinize Fig. 6. There are three general aspects that merit emphasis. The first aspect is the occurrence of a minimum $T_\Lambda^{\min} = 50315$ K at $T_A^{\min} = 1100$ K. Recalling, by definition,

$$T_\Lambda = \frac{Z_0^2 L_B X^2 e^{-\kappa}}{k_B}, \quad (33)$$

it implies that, for given κ, Ψ , and η_c , there exists a minimum σ_0 below which no liquid-liquid phase separation is anticipated. For the Belloni model, the set of values ($\eta_c = 0.3137$, $\Psi = 25$ mV, $T_0 = 293$ K, and $\epsilon = 78.5$) yields $\sigma_0^{\min} = 5120$ Å, which is slightly larger than the $\sigma_0^{\min} = 5095$ Å in the DLVO model. At this σ_0^{\min} , the Hamaker constant is $A = 1.518 \times 10^{-20}$ J. At this point, it is perhaps worthwhile to enquire if the present T_Λ vs T_A curve has any relevance to previous experiments. As pointed out above, the one early experiment on charged spherical colloids in water whose colloidal conditions closely mimic the present theory is that of Kotera, Furusawa, and Kubo [9]. We now discuss the experimental findings of the latter work and see if these results can be correlated with the presently obtained T_Λ vs T_A curve. In their colloid chemical studies of polystyrene latices, Kotera, Furusawa, and Kubo appealed to the optical and microscopic methods, and investigated the effect of the second minimum on the colloidal stability for a series of “soap-free” polystyrene latex particles varying in $\sigma_0(\Psi)$ from 3500 Å (23 mV) to 13740 Å (29 mV). They determined the critical flocculation concentration of KCl for each σ_0 using the transmission coefficient of light as well as microscopy, and found that the critical flocculation concentration varies anomalously with the σ_0 and Ψ . In consultation with two earlier publications [21,25] (see also Ref. [10] for a

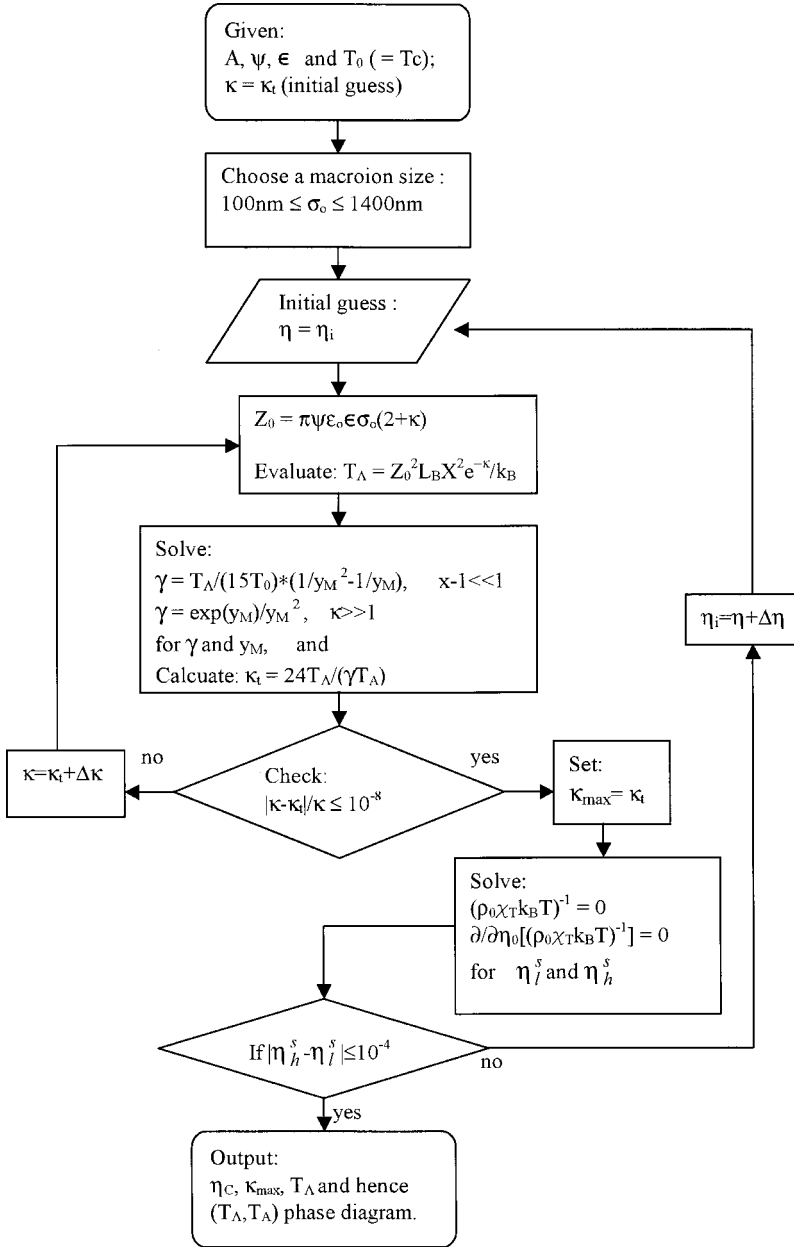


FIG. 5. Flow chart showing the numerical procedure that leads to the determination of the T_{Λ} vs T_A . Self-consistency in obtaining the κ_{\max} and the η dependence in T_{Λ} have been fully considered.

more recent discussion on the A of the polystyrene-water mixture), these authors proposed $A = 1.3 \times 10^{-20}$ J for their measured polystyrene-water system. Using their measured data for the σ_0 , Ψ , and critical flocculation concentration, we plot in Fig. 7 the change of $V(x)$ function with σ_0 . A striking characteristic of these $V(x)$ can be recognized. In going from $\sigma_0 = 3500$ Å to 13 740 Å, it is clearly seen that the $V(x)$ varies from a shallow second minimum $V(x_m)$ accompanied by a lower $V(x_M)$ (for $\sigma_0 \leq 4000$ Å) to a deeper $V(x_m)$ accompanied by a higher $V(x_M)$ (for $\sigma_0 > 5000$ Å). In particular we notice that the $V(x_m)$ for the case $\sigma_0 \leq 4000$ Å is located at $x_m \approx 1.04$ [26] somewhat farther than $x_m \approx 1.004$ for the case $\sigma_0 > 5000$ Å. Based on their analysis of the time-variation curves of transmission coefficients for the latex particles, Kotera, Furusawa, and Kubo conjectured the “crossover” σ_0 , which differentiates an irreversible coagulation phase from that of a reversible coagulation, lying

roughly in the range 7000–8000 Å. Referring to Fig. 8 for the σ_0 vs T_A stability curve, at the value $A = 1.3 \times 10^{-20}$ J, which corresponds to $T_A = 942$ K, the corresponding $T_{\Lambda} = 50\,691$ K yields immediately $\sigma_0^{\min} = 5152$ Å, at which place $\kappa_{\max} = 374.7$. This σ_0^{\min} is lower than the range of σ_0 values noted above. We should remark, however, that the σ_0^{\min} deduced here is fixed at $\Psi = 25$ mV and is not exactly the same as those given in Kotera, Furusawa, and Kubo’s work. In fact the Ψ in Kotera, Furusawa, and Kubo’s experiments increases gradually with σ_0 . As clearly displayed in Fig. 7, such changes in Ψ will tend to raise the potential barrier $V(x_M)$ [3] accompanied by a deepening of $V(x_m)$ due to the σ_0 increment. Nevertheless, it is encouraging to note that our theory predicts a $\sigma_0^{\min} = 5152$ Å below which an irreversible coagulation sets in. This feature is consistent with the experimental observation of Kotera, Furusawa, and Kubo where both aqueous polystyrene lattices $\sigma_0 = 3500$ Å and σ_0

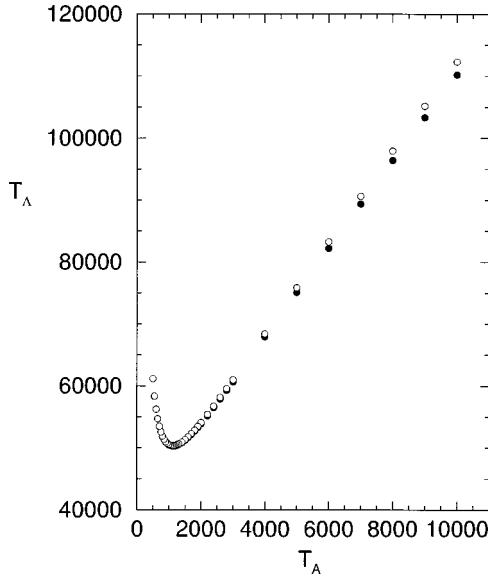


FIG. 6. Plot of T_Λ vs T_A for an aqueous charged colloidal dispersion calculated at $T_0 = T_c = 293$ K and for $V(x_M) = 15 k_B T$ (see text). Notations: Belloni, closed circles; DLVO, open circles.

$= 4160 \text{ \AA}$ were found to exhibit irreversible coagulations as confirmed from an analysis of the time variation of the transmission coefficients.

The second aspect of the T_Λ vs T_A curve is its prediction of an interesting coagulation feature for a monodisperse charged colloidal dispersion. Stipulating a given σ_0 , 6000 \AA say, in the range $5120 < \sigma_0 < 6200 \text{ \AA}$ [27], which corresponds to $T_\Lambda = 58320$ and 59209 in the Belloni model, Fig. 9 reveals the fact that the agglomeration phenomenon can be

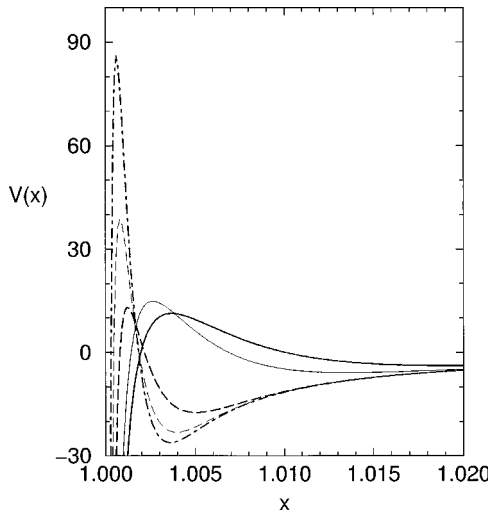


FIG. 7. Intercolloidal particle potential function $V(x)$ (in units of $k_B T$) vs $x = r/\sigma_0$ calculated using the DLVO repulsive part plus Eq. (10) at temperature $T = 293$ K for polystyrene colloids with $\sigma_0 = 3500 \text{ \AA}$ (thick-full curve), 4160 \AA (thin-full curve), 7580 \AA (thick-dashed curve), 10780 \AA (thin-dashed curve), and 13740 \AA (chain curve). The reduced critical flocculation concentrations κ and surface potentials Ψ are (214.1, 302.4, 746.1, 1011.7, 1188.9) and (23, 25, 27, 28, 29 mV), respectively. The Hamaker constant is taken to be $1.3 \times 10^{-20} \text{ J}$ for all σ_0 .

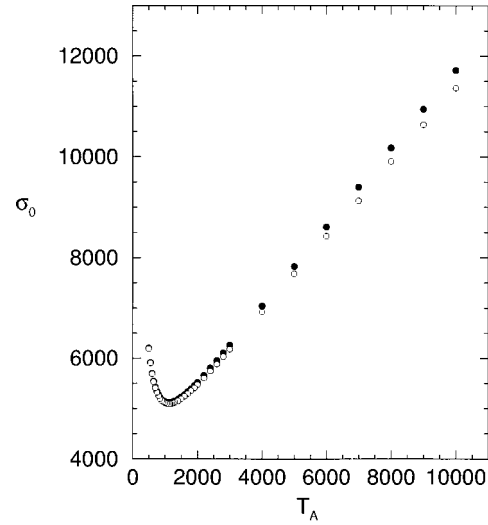


FIG. 8. Plot of macroion size σ_0 vs T_A for an aqueous charged colloidal dispersion calculated at $T_0 = T_c = 293$ K and for $V(x_M) = 15 k_B T$ (see text). Notations: Belloni, closed circles; DLVO, open circles.

realized in an aqueous monodisperse charged colloid composed either of a higher density ($\eta_c = 0.4775$) colloidal particles dispersed in a dielectric medium characterized by a smaller A ($0.7355 \times 10^{-20} \text{ J}$) or of a lower density ($\eta_c = 0.1961$) colloidal liquid having a larger A ($3.679 \times 10^{-20} \text{ J}$). Since the Hamaker constant sensitively reflects the depth of the second minimum [9,10] as does the electrolyte concentration, it would be a challenging experimental endeavor to explore the ease of observing the weak

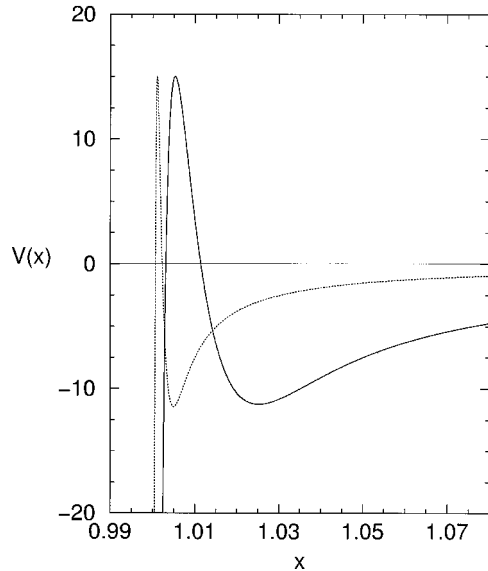


FIG. 9. Intercolloidal particle potential function $V(x)$ (in units of $k_B T$) vs $x = r/\sigma_0$ calculated using the Belloni model for the repulsive part plus Eq. (10) for charged colloids with $\sigma_0 = 6000 \text{ \AA}$ at temperature $T = 293$ K. The stability ‘‘points’’ for the same σ_0 , which can be read from Fig. 8, are $A = 3.679 \times 10^{-20} \text{ J}$, $\eta_c = 0.1961$, $\kappa_{\max} = 157.2$ (thick-full line); $A = 0.736 \times 10^{-20} \text{ J}$, $\eta_c = 0.4775$, $\kappa_{\max} = 800.7$ (thin-full line).

reversible coagulation for monodisperse charged colloidal solutions at these A and to understand the experimental results from the theoretical model (compare, for example, the $V(x)$ depicted in Fig. 9 for these colloidal conditions). Such experimental setups should not be too difficult to accomplish.

The third aspect is the much less likelihood for a charged colloidal dispersion to undergo the liquid-liquid phase separation if its Hamaker constant $A < 0.53 \times 10^{-20}$ J, for the A in this region, has already assumed $\eta_c > 0.5$, which is the regime of solid phase. If one were to accept the range of A spanning $0.5 \times 10^{-20} \text{ J} \leq A \leq 5 \times 10^{-20} \text{ J}$ to be experimentally accessible and to confine our study to a fixed $\Psi \leq 25$ mV, there then exist lower limit of σ_0^{min} values (along the coagulation stability curve given by Figs. 6 or 8) serving the boundary between the irreversible ($\sigma_0 < \sigma_0^{\text{min}}$) and weak reversible ($\sigma_0 \geq \sigma_0^{\text{min}}$) coagulations. To keep within this range of A for a larger σ_0 , one would generally have to increase Ψ (> 25 mV) in order to simulate a higher potential barrier [since the $V(x_M)$ decreases with increasing σ_0 but it increases with increasing Ψ [3]].

IV. CONCLUSION

We draw attention to a realistic statistical-mechanics model suitable for delineating the structures and the thermodynamics of concentrated charged colloidal dispersions. Differing from the usual DLVO model, the model is valid for any finite concentration of macroions. The model is therefore physically appropriate for describing the liquid-liquid phase separation corresponding to a lower- and a higher-density liquid phase. After justifying the validity of the model within the MSA OZ integral equation approach, we proceed to set up an effective two colloidal particle interaction, which is theoretically more general than the usual DLVO model. Following Victor and Hansen, we apply the Weeks-Chandler-Andersen perturbation theory to construct the Helmholtz free energy to first-order correction. The calculated pressure, chemical potential, and related thermodynamic functions afford the determination of critical points, the η_c and the κ_c , and hence the spinodal decomposition and the liquid-liquid coexistence curves. We summarize our theoretical findings as follows.

(1) The calculated spinodal decomposition and liquid-

liquid coexistence curves within the Belloni model show a shift in κ_c to lower values and enclose a larger area compared with the DLVO model.

(2) For an excess salt concentration $\kappa \leq 200$, the quantities indicated in point (1) using the Belloni model differ larger from those obtained by the DLVO model, whereas for $\kappa > 300$ the differences in the corresponding results between the two models are smaller.

(3) The stability curve determined in the Belloni model, which marks a separation of an irreversible and a reversible coagulation for aqueous charged colloids near room temperature, predicts a minimum size of approximately 5000 Å, which is quite consistent with early experiments reported by Kotera, Furusawa, and Kubo who observed, from an analysis of the time variation of transmission coefficients, an irreversible coagulation for two aqueous polystyrene lattices whose macroion sizes are $\sigma_0 = 3500$ Å and $\sigma_0 = 4160$ Å.

(4) For any monodisperse charged colloids whose macroion size falls into range $5120 < \sigma_0 < 6200$ Å, it is possible to observe the coagulation phenomenon characterized by either a higher-density colloidal dispersion having a smaller A or a lower-density colloidal solution pertaining to a larger A .

(5) For an aqueous charged colloidal dispersion, our thermodynamic perturbation theory disallows the Hamaker constant $A < 0.53 \times 10^{-20}$ J for observing the liquid-liquid phase separation, because in this region the system has already had $\eta_c > 0.5$ and hence has moved into a solid phase.

ACKNOWLEDGMENTS

This work was supported in part by the National Science Council (NSC89-2112-M-008-064). S.K.L. would like to thank the Royal Society, UK and the NSC, Taiwan for an opportunity to participate in an exchange program (NSC89-2911-I-008-008-2) during which period the final part of this manuscript was written. S.K.L. would like to express his gratitude to Professor P. A. Madden for hosting his visit to Oxford University and to thank Professor F. Sciortino and Professor C. H. Oh for their kind hospitality during his subsequent visits at the Università di Roma ‘La Sapienza’ and National University of Singapore, respectively. Finally, S.K.L. acknowledges partial support from Professor W. H. Ip, Dean of the Faculty of Science, NCU for his visit to NUS.

-
- [1] L. Belloni, *J. Chem. Phys.* **85**, 519 (1986).
 [2] S. Khan, T. L. Morton, and D. Ronis, *Phys. Rev. A* **35**, 4295 (1987).
 [3] E. J. Verwey and J. G. Overbeek, *Theory of the Stability of Lyophobic Colloids* (Elsevier, Amsterdam, 1948).
 [4] S. K. Lai and G. F. Wang, *Phys. Rev. E* **58**, 3072 (1998).
 [5] S. K. Lai, J. L. Wang, and G. F. Wang, *J. Chem. Phys.* **110**, 7433 (1999).
 [6] G. F. Wang and S. K. Lai, *Phys. Rev. Lett.* **82**, 3645 (1999).
 [7] J. H. Schenkel and J. A. Kitchener, *Trans. Faraday Soc.* **56**, 161 (1960).
 [8] J. A. Long, D. W. J. Osmond, and B. Vincent, *J. Colloid Interface Sci.* **42**, 545 (1973).
 [9] A. Kotera, K. Furusawa, and K. Kubo, *Kolloid Z. Z. Polym.* **240**, 837 (1970).
 [10] K. Gotoh, R. Kohsaka, K. Abe, and M. Tagawa, *J. Adhes. Sci. Technol.* **10**, 1359 (1996).
 [11] M. J. Grimson, *J. Chem. Soc., Faraday Trans. 2* **79**, 817 (1983).
 [12] J. M. Victor and J. P. Hansen, *J. Phys. (France) Lett.* **45**, L307 (1984); *J. Chem. Soc., Faraday Trans. 2* **81**, 43 (1985). There are errors in the appendix of the second reference; the $\alpha(\eta)$

should have a numeric constant four in the first integral, and the second, third, and fourth integrals all should be corrected by a minus sign in front.

- [13] J. Kaldasch, J. Laven, and H. N. Stein, *Langmuir* **12**, 6197 (1996).
- [14] Here we are concerned with the second minimum of $V(r)$ whose interaction strength comes solely from the London-van der Waals attraction. The physical origin and the range of the latter attraction are somewhat different from many other mechanisms [see Löwen, *Physica A* **235**, 129 (1997) for a general description] giving rise to different ranges of attractive forces. Since the mechanism leading to the attraction varies with physical systems under different physical conditions and is still not fully understood or may be even controversial, we confine our calculations to only the van der Waals kind of attraction. Note that, depending on the colloidal conditions, the range of the London–van der Waals attraction for charged colloids may be short ranged but it is of a somewhat different nature from those extremely short-ranged attractions that are shown theoretically [J. M. Kincaid, G. Stell, and E. Goldmark, *J. Chem. Phys.* **65**, 2172 (1976); C. F. Tejero *et al.*, *Phys. Rev. Lett.* **73**, 752 (1994)] and in computer simulation studies [B. Alder and D. Young, *J. Chem. Phys.* **70**, 473 (1979); P. Bolhuis and D. Frenkel, *Phys. Rev. Lett.* **72**, 2211 (1994)] to lead to a different type of phase transition—the isostructural solid–solid transition.
- [15] J. D. Weeks, D. Chandler, and H. C. Andersen, *J. Chem. Phys.* **54**, 5237 (1971).
- [16] A. Adelman, *Chem. Phys. Lett.* **38**, 567 (1976); *J. Chem. Phys.* **64**, 724 (1976).
- [17] D. A. McQuarrie, *Statistical Mechanics* (Harper and Row, New York, 1976), pp. 266.
- [18] L. Verlet and J. J. Weis, *Mol. Phys.* **24**, 1013 (1972).
- [19] J. P. Hansen, L. Reatto, M. Tau, and J. M. Victor, *Mol. Phys.* **56**, 385 (1985).
- [20] We have not included the additional contributions coming from the so-called volume terms. The reason is that under an excess salt condition (~ 0.01 M) these volume terms are small or nearly constant and would be inconsequential [see, for example, R. van Roij and J. P. Hansen, *Phys. Rev. E* **59**, 2010 (1999) and R. van Roij and R. Evans, *J. Phys.: Condens. Matter* **11**, 10047 (1999)] in the calculated phase separation boundary of the low- and high-density liquids. Several early [B. D. S. Derek, Y. C. Chan, and D. J. Mitchell, *J. Colloid Interface Sci.* **105**, 216 (1985); M. J. Grimson and M. Silbert, *Mol. Phys.* **74**, 397 (1991)] and recent [R. van Roij and J. P. Hansen, *Phys. Rev. Lett.* **79**, 3082 (1997); M. Dijkstra and R. van Roij, *J. Phys.: Condens. Matter* **10**, 1219 (1998); A. R. Denton, *ibid.* **11**, 10061 (1999); *Phys. Rev. E* **62**, 3855 (2000); H. Graf and H. Löwen, *ibid.* **57**, 5744 (1998); P. B. Warren, *J. Chem. Phys.* **112**, 4683 (2000)] works have given rather lengthy discussions on the consequence of these volume terms, but in one way or another these studies have shown that their effects are seen to be significant mainly at extremely low electrolyte concentrations ($\sim \mu\text{M}$). The interested readers are referred to these works for further details.
- [21] A. Watillon and A. M. Joseph-Petit, *Discuss. Faraday Soc.* **42**, 143 (1966).
- [22] J. Th. G. Overbeek, *Colloid Science*, edited by H. R. Kruyt (Elsevier, Amsterdam, 1948).
- [23] Contrary to the remark made by Victor and Hansen [12], we find the stipulation of the potential barrier $V(x_M)$ sensitive to the results predicted. For example, we obtain a σ_0^{min} (see the discussion below) lower by about 500 \AA if we choose $V(x_M) \approx 10 k_B T$.
- [24] J. Visser, *Adv. Colloid Interface Sci.* **3**, 331 (1972).
- [25] R. H. Ottewill and J. N. Shaw, *Discuss. Faraday Soc.* **42**, 154 (1966).
- [26] This x_m is compatible with the experimental data of Watillon and Joseph-Petit [21]. Employing their measured data ($\sigma_0 = 1760 \text{ \AA}$, $A = 0.5 \times 10^{-20} \text{ J}$, $18 < \Psi < 30 \text{ mV}$, and $150 < \kappa < 303$) for the aqueous polystyrene lattices, we have checked that the average x_m for different concentrations of NaClO_4 is located approximately at $x_m \approx 1.024$, which is reasonably close to the value expected for the σ_0 range.
- [27] We base our argument on setting $V(x_M) = 15 k_B T$. One should bear in mind an order of approximately 500 \AA for a change in setting of $V(x_M)$ by about $5 k_B T$ (see the comment in Ref. [23]).